iScience

CellPress
OPEN ACCESS

Article

Naphthalimide-based light-induced nitric oxide-releasing nanoscale vesicles with visual detection and cytotoxicity studies

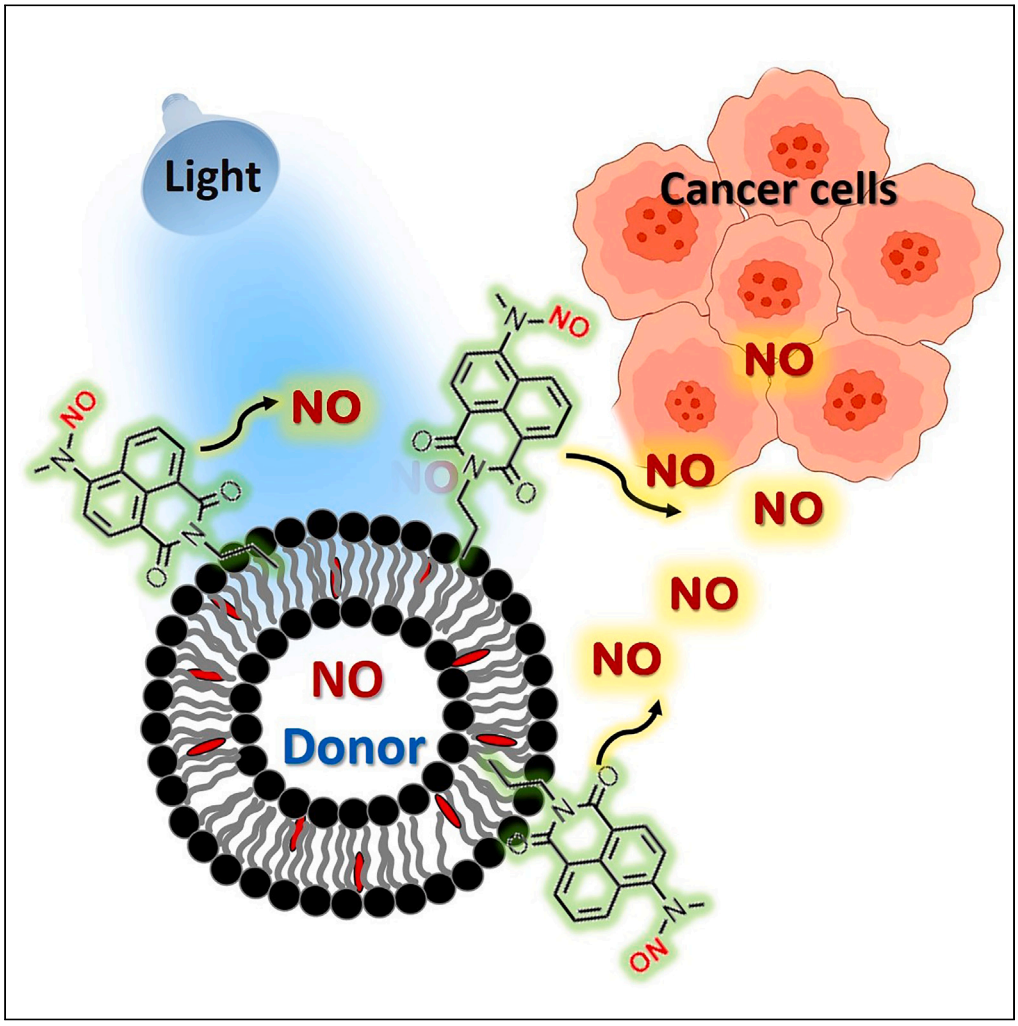

Vinod Kumar, Kanika, Nitin, Nancy Sharma, Rahul, Rehan Khan, D. Amilan Jose

amilanjosenit@nitkkr.ac.in

Highlights

Amphiphilic N-nitroso compound (**Nap-NO**) for the light-controlled release of NO

NO release from nanoscale liposomes modulated by lipid fluidity

Nap-NO incorporated alginate polymer beads offers visual detection of NO release

Liposomes co-embedded with Nap-NO exhibit cytotoxic effect to cancer cells

Kumar et al., iScience *27*, 110230
July 19, 2024
https://doi.org/10.1016/j.isci.2024.110230

iScience

CellPress
OPEN ACCESS

Article

Naphthalimide-based light-induced nitric oxide-releasing nanoscale vesicles with visual detection and cytotoxicity studies

Vinod Kumar,[1] Kanika,[2] Nitin,[1] Nancy Sharma,[1] Rahul,[1,2,3] Rehan Khan,[2] and D. Amilan Jose[1,4,*]

SUMMARY

The therapeutic potential of nitric oxide (NO) has been receiving increasing interest, but achieving controlled release under physiological conditions remains challenging. Herein, we report a colorimetric and fluorescence responsive naphthalimide-based amphiphilic N-nitroso-based NO donor (Nap-NO) and its NO-releasing behavior. Nap-NO was incorporated into phospholipid nanovesicles to make it biocompatible and water-soluble. Light-induced NO-releasing behavior and emission changes were monitored via UV-vis, colorimetric detection, IR (Infrared) spectroscopy studies, and Griess assay. The Nap-NO donor within the 1,2-dioleoyl-*sn*-glycero-3-phosphocholine (DOPC)-cholesterol vesicles exhibited a slower release rate, with a significantly extended half-life as compared to the only DOPC vesicles. Incorporating the Nap-NO into alginate hydrogel beads enables a simple, visual detection of NO release through color and emission changes. Bioimaging experiments within the HCT cell line reveal the use of the new NO donor for fluorescent bio-imaging and clearly illustrate their proficiency in killing cancer cells upon NO delivery in the presence of light.

INTRODUCTION

Nitric oxide (NO), a small molecule with profound biological significance, has garnered substantial attention for its versatile role as a signaling molecule in various physiological and pathological processes.[1–4] NO improves cardiac health, reduces high blood pressure, reduces erectile dysfunction, and improves healing processes and respiratory response. Harnessing the therapeutic potential of NO, however, has been challenged by its short half-life, reactivity, and limited bioavailability in biological systems.[4] In the search for effective NO delivery systems, researchers have explored diverse strategies, such as up-conversion nanoparticles, nanovesicles, micelles, quantum dots, graphene-based quantum dots, nanosheets, and lipid vesicles based NO donors.[2,5,6] Among these, the integration of NO-releasing compounds into lipid-based vesicular systems has emerged as a promising avenue. N-Diazeniumdiolates (NONOates)[7–10] and S-nitrosothiols (RSNOs)[11–15] are the most widely used categories of NO donors due to their ability to spontaneously release NO in physiological media. NONOates undergo spontaneous decomposition via hydrolysis under physiological conditions. However, the uncontrolled NO release from NONOates and RSNOs leads to limited bio-medical application. But for the potential applications of NO in cancer gas therapy, the development of a controlled NO release system is of utmost importance.

Light-controlled release of NO donors can reach controllable and precise release in a temporal and spatial-controlled manner. It leads to the development of various light controlled NO delivery system including metal nitrosyl complexes and organic NO donors.[16–19] Among various types of NO-releasing compounds N-nitrosated organic compounds are well known for light activated NO release.[20–22] In this regard, N-nitrosated derivatives of naphthalic 1,8 anhydride, have gathered attention due to their capacity to release NO upon exposure to light irradiation with drastic changes in emission and colorimetric response. In the presence of light, these compounds transform to form anilinyl radical as a byproduct and undergo *in situ* reduction, to form 4-amino naphthalimides as a fluorescence compound,[23] which can serve as an effective fluorescent indicator to monitor the release of NO, with no apparent changes in the absence of light. Nevertheless, as like many other organic NO-donors, N-nitrosated derivatives of naphthalic anhydride lack water solubility which restricts the use of these compounds in biological applications. Most of the organic NO donors use DMSO as a cosolvent for the NO-releasing studies; introduction of these compounds into the liposomal system may enhance their water solubility, increase drug loading, minimize toxicity to the cells, and allow a controlled release at physiological condition. Recently, we have also shown the advantage of liposomes for NO-releasing system.[24–26] NO-donors may be encapsulated[27] or incorporated into the liposomes, but encapsulation may have the disadvantage of separation and

[1]Department of Chemistry, National Institute of Technology Kurukshetra, Kurukshetra 136119, Haryana, India
[2]Chemical Biology Unit, Institute of Nano Science and Technology (INST), Knowledge City, Sector 81, Mohali, Punjab 140306, India
[3]Present address: Department of Chemistry, Malaviya National Institute of Technology, Jaipur, Rajasthan 302017, India
[4]Lead contact
*Correspondence: amilanjosenit@nitkkr.ac.in
https://doi.org/10.1016/j.isci.2024.110230

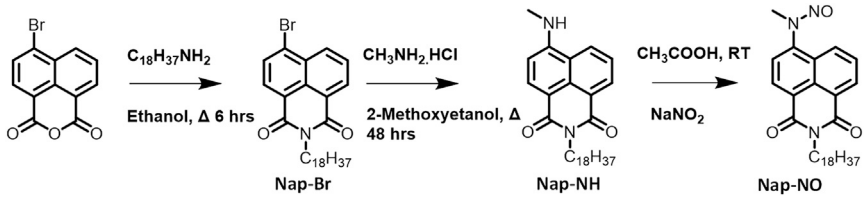

Scheme 1. Schematic representation for the synthesis of Nap-NO

purification to remove solute that might have permeated the lipid membrane and long-time stability.[28] Therefore, incorporating amphiphilic NO donors into the vesicles may be advantageous.

Herein, we report the synthesis and characterization of a naphthalimide based new amphiphilic N-nitroso-based NO donor Nap-NO. To make the compound biocompatible, nanosized vesicles composed of 1,2-dioleoyl-*sn*-glycero-3-phosphocholine (DOPC) and cholesterol embedded with Nap-NO were prepared. The use of co-solvent DMSO is not required at liposome-based NO-releasing system, which is required for therapeutic applications. This also eliminates potential concerns associated with solvent toxicity and simplifies the translation of our technology into clinical applications. Also, the NO release kinetic can be modulated easily by adjusting vesicle composition with cholesterol and the amount of NO-donor loading. NO donor Nap-NO was also incorporated into alginate-based hydrogel beads for the controlled release of NO. Light-responsive behavior of alginate beads offers a versatile platform for controlled NO delivery with a real-time visual monitoring by color and emission change. Furthermore, the non-toxic behavior of the new NO-releasing system before and after the release was confirmed by conducting cytotoxicity assessments on HCT cell lines. The Nap-NO incorporated vesicles induced the cell death of cancer cells by NO within the cells upon blue light irradiation. Further, real-time cell images through the emission of naphthalimide fluorophore were achieved through direct excitation of the NO-donor in cells.

RESULTS AND DISCUSSION

Synthesis and NO-release studies of NAP-NO

N-Nitroso compounds are well-known as NO-releasing molecules and the homolysis of N-N bond can occur even at mild conditions. This inspired us to design a new amphiphilic N-nitroso-based NO donor. N-Nitroso derivative of amphiphilic naphthalic-1,8-anhydride (*Nap-NO*) was synthesized by three step reaction as shown in Scheme 1 (Figures S1–S9).

New NO donor Nap-NO shows characteristic UV-vis absorption peaks at 237 nm and 347 nm in DMSO/water (20/80) mixture. As expected, Nap-NO did not show any fluorescence upon excitation at 440 nm, emission was completely OFF stage. However, upon irradiation with blue light, the increase in fluorescence emission at 535 nm was observed due to the break in the N–NO bond of the N-nitroso group and the release of NO (Figure 1B). This increase in fluorescence emission is attributed to the turn-on photoinduced electron transfer (PET) mechanism, which is initially hindered by the presence of attached NO. Further, the absorption peak at 347 nm diminishes, and a new absorption peak emerges at 260 nm, 285 nm, and 433 nm when exposed to blue light (420 nm, 3W) for 30 min. The change in the UV-vis absorption is attributed to the conversion of N–NO to N–H. Based on the change absorption spectrum with time under light, the reaction rate for NO release was estimated as 0.0397 min^{-1}, with a half-life of 1.8 min. The photochemical quantum yield of this process was estimated as 130.6 × 10^{-3} (SI page no. S13 and S14)

The fluorescent photodecomposition product from Nap-NO was further confirmed using IR studies. A new IR peak responsible for -NH stretching appeared at 3,371 cm^{-1} upon photodecomposition; this confirms the release of NO from the Nap-NO (Figure S10). As Nap-NO has limited solubility in water, the NO release studies were performed in DMSO/water (20/80).

Preparation and analysis of NAP-NO co-embedded vesicles

The NO-release behavior in organic solvents and semi-aqueous solution has its own disadvantages that limits the potential of NO photodonor for biomedical and therapeutic applications. Recently, Zhang et al. utilized the N-nitrosated napthalimides for NO release that is triggered by UV light at 365 nm or a two-photon laser at 740 nm.[22] Nevertheless, this report uses DMSO as a co-solvent for the biological studies. Also, small molecules have low bioavailability, less stability, and lack site specificity. To overcome this limitation, the advantages of vesicles/liposomes were explored. Liposomes are bio-compatible and excellent platforms for drug delivery,[29] therefore Nap-NO was incorporated into the phospholipid-based vesicles to enhance biocompatibility and water solubility. A thin film hydration approach[30] was used to prepare nanoscale vesicles incorporating Nap-NO.[31] This involved mixing commercially available phospholipids such as DOPC, cholesterol (to provide rigidity to the bilayer), and NO donor Nap-NO (10 mol % relative to DOPC) in a 10 mM HEPES buffer at pH 7.4. Nap-NO incorporated vesicular lipid bilayers **Nap-No.Ves** and Nap-NO.Cho were prepared by well-established procedure, including homogenization through extrusion with a 100 nm polycarbonate membrane[32] (see experimental model and study participant details section). The mean particle size of the vesicles is estimated as 90 nm ± 16 nm with average Pdi of 0.139 assessed from four independent DLS experiments (Table S1). Transmission electron microscopy (TEM) and scanning electron microscopy (SEM) images provided visual evidence that the Nap-NO incorporated vesicle solution containing is spherical and has a mixture of large and small vesicles in the size range of 100–150 nm (Figures 2A and

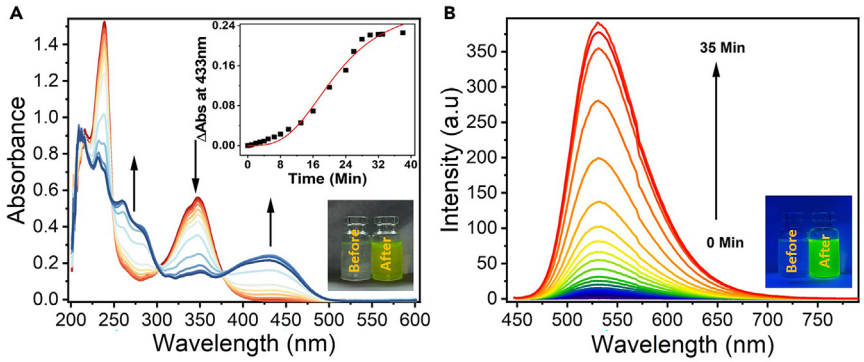

Figure 1. UV-visible absorption spectra and emission spectra of Nap-NO with blue (420 nm 3W) light irradiation

(A) Change in absorption spectra of Nap-NO in DMSO/water (20/80) with blue light irradiation (420 nm 3W) from 0 to 35 min (excitation = 440 nm).

(B) Change in emission spectra of Nap-NO (40 μM) in DMSO/water (20/80) with blue light irradiation (420 nm 3W) from 0 to 35 min.

2B). The incorporation of Nap-NO into the vesicle was confirmed through UV-vis spectroscopy, where the absorption maximum at approximately 350 nm closely matched the absorption spectrum of Nap-NO in organic solution (Figure S11). The vesicles are stored under dark and remained stable in the absence of light for up to 7 days. Vesicles stored under day light conditions are unstable and precipitated over 48 h of time. It is also observed that the dilution of the vesicle stock solution did not significantly alter the vesicle size (Figure S12).

NO-release studies of liposomes

NO-releasing behavior of liposomes **Nap-NO.Ves** was monitored by irradiation with blue light (420 nm, 3W). Time-dependent UV-vis and emission spectra of **Nap-NO.Ves** were monitored upon irradiation with light (Figure S13). The spectral changes are very similar to that of *Nap-NO* in DMSO/water mixture. The rate for NO release from the vesicular medium is found to be 0.34 min^{-1} and a half-life is calculated as 2.03 min. The quantum yield estimated is 3.74×10^{-3}. It was observed that the release of NO from the nano-scale vesicular medium **Nap-NO.Ves** is slower as compared to Nap-NO in the aqueous-organic medium. The rate of NO release from Nap-NO is slowed by incorporating in the lipid bilayer membrane.

Cholesterol is frequently used in the formulation of liposomes. Cholesterol on the lipid bilayer membrane is known to provide membrane rigidity, preventing vesicle aggregation and fusion. DOPC exists in a fluid state, the addition of 30 mol % of cholesterol leads to a decrease in the fluidity of DOPC lipid and also an increase in the stability of the liposomes.[33] Therefore, to increase the stability of liposomes, Nap-NO was mixed with cholesterol (30 mol %) and new liposomes Nap-NO.Cho was prepared (Scheme 2). It is observed from DLS and UV-vis studies that the stability of the liposomes with cholesterol (Nap-NO.Cho) is much better, stable up to 15 days as compared **Nap-NO.Ves** having no cholesterol (Figures S14 and S15). The fluorescence turn-on assay revealed that NO-triggered fluorescence occurred equally effective in both cholesterol-containing and cholesterol-free vesicles.

NO-releasing behavior of Nap-NO.Cho was also monitored by UV-vis and emission spectra in the presence of light. Time-dependent NO release studies revealed that change in absorbance and emission spectra were similar to the changes observed for **Nap-NO.Ves**. Based on the time-dependent spectral change studies (Figure S16), the rate of NO release was observed as 0.20 min^{-1} and a half-life was calculated as 3.36 min. The quantum yield was measured as 4.39×10^{-3}. These results reveal that the rate of NO from Nap-NO.Cho is slower as compared to **Nap-NO.Ves**. So, the vesicular system can be used for the slow and steady release of NO as compared to Nap-NO.

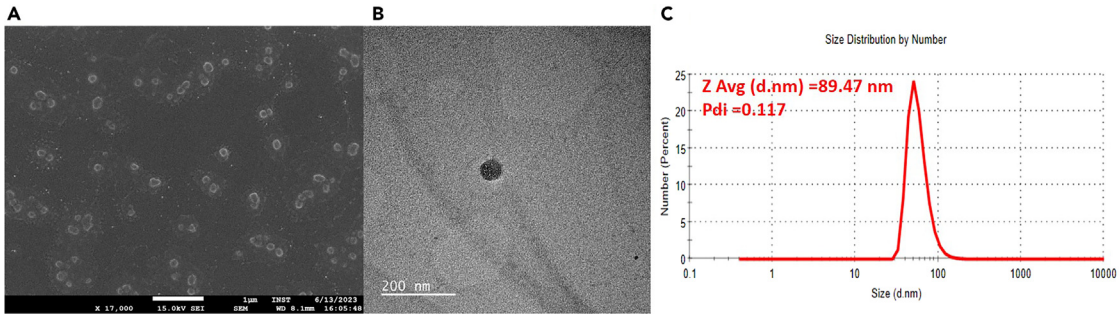

Figure 2. Characterization of nanoscale liposomes

(A) SEM and (B) TEM images of **Nap-NO.Ves**.

(C) DLS (dynamic light scattering) data of **Nap-NO.Ves**.

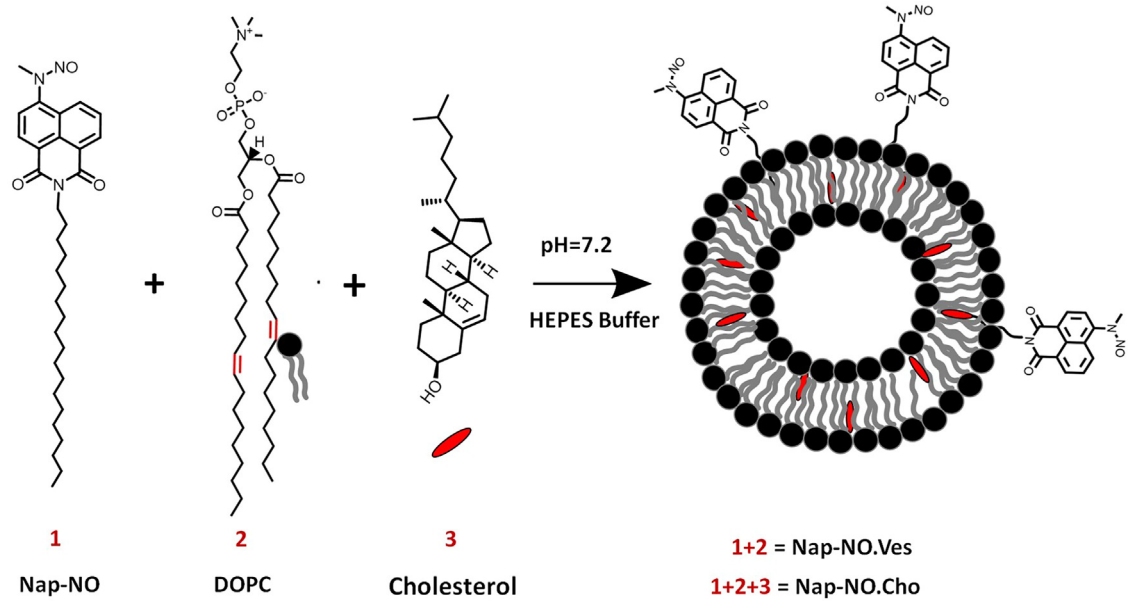

Scheme 2. Schematic representation of nano vesicles Nap-NO.Ves and Nap-NO.Cho prepared by DOPC and cholesterol combination system

The rate of NO release from all three NO-releasing systems is summarized in Table 1. It shows that the rate of NO release from the amphiphilic compound Nap-NO is very fast in aqueous organic solvent mixture (DMSO/H_2O). But after incorporating Nap-NO into the lipid vesicular system, the rate of NO release becomes slow. Interestingly, comprising 30% cholesterol on the liposomes even further slows down the rate of NO release. The half-life ($t_{1/2}$) of Nap-NO.Cho was longer (3.36 min) as compared to that of **Nap-NO.Ves** (2.03 min), indicating relatively slower NO release in the liposom system having cholesterol. Cholesterol increases the lipid-packing density, significantly increasing the order of the lipid packing, and maintains high membrane fluidity.[34] The effect of lipid fluidity on NO release and other analytes is already described in the literature.[25,35] Therefore, the addition of 30 mol % cholesterol to DOPC lipid influences NO release rate. This result emphasizes the impact of the surrounding medium on NO-release kinetics. Furthermore, this observation indicates the pivotal role of lipid-based vesicular systems for the controlled slow NO release, specifically DOPC-cholesterol, in enhancing the stability and bioavailability of NO-releasing compounds.

Further, to quantify and confirm the NO release from the NO-releasing systems, a colorimetric Griess assay was performed (Figure 3A). This assay confirms the NO release through the formation of a chromophoric azo derivative, which shows a typical UV-vis absorbance band at 540 nm along with a noticeable color change. This assay validates the NO release from Nap-NO and **Nap-NO.Ves**. The release of NO in **Nap-NO.Ves** was dependent on vesicle concentration, allowing for controlled modulation of NO release by varying the vesicle solution concentration (Figure S17). The amount of NO released from NO donor **Nap-NO.Ves** (16 μM) was estimated by Griess assay. It was calculated to be 6.21 μM, which is well in the range of non-toxic levels used in therapeutic applications.

Further, the role of light on the release of NO from the NO-releasing systems was confirmed by alternative light ON and OFF experiments. As shown in Figure 4, the changes in absorbance and emission intensity were observed only in the presence of light. This experiment illustrated the use of light for the controlled release of efficient NO release only in the presence of light.

Real-time visualization of NO release from hydrogel beads

Turn-on colorimetric and fluorescent response would allow easy visualization of NO release in solutions and cellular targets. Hydrogel-based soft materials provide a steadier release of NO and have more advantages to medicinal applications due to their tissue-like nature and hydrophilic properties.[36] Recently, NO-releasing hydrogels have been explored for various therapeutic applications such as wound healing,

Table 1. Rate, half-life ($t_{1/2}$), and quantum yield of NO released from different composition of NO-donors

	NO releasing system	Rate (min^{-1})[a]	Half-life (min)[a]	Quantum yield[a]
1.	Nap-NO (40 μM)	0.40 ± 0.03	1.78	0.13
2.	**Nap-NO.Ves** (16 μM)	0.34 ± 0.03	2.03	0.0037
3.	Nap-NO.Cho (16 μM)	0.20 ± 0.04	3.36	0.0044

[a]Value mentioned here is the average of three independent measurements.

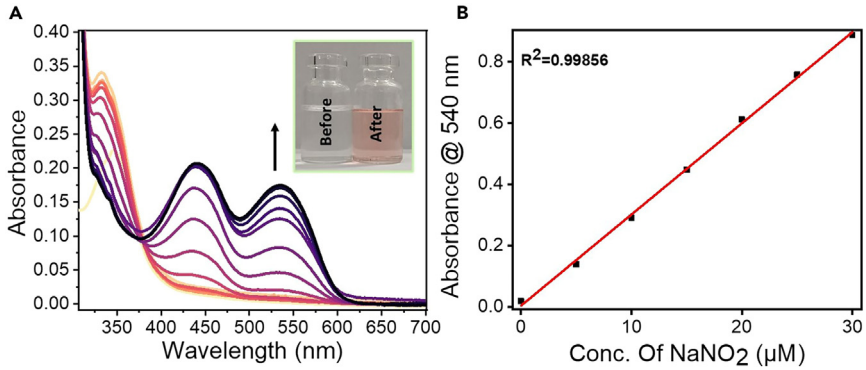

Figure 3. Griess assay for the quantification of nitric oxide

(A) Change in absorption spectra of **Nap-NO.Ves** (16 μM) in presence of modified Griess reagent (10 mM HEPES buffer, pH 7.2).

(B) Standard curve using $NaNO_2$ solution (5–50 μM) for the quantification of Greiss assay. Linear range: 0–30 μM.

possible angiogenic therapy, antimicrobial effect, cardiovascular therapy, vasodilative potential, and stem cell differentiation.[36] However, NO-releasing hydrogels that can show visual changes upon NO release are rare.

Alginate beads are tiny spherical structures with a fascinating range of applications across various fields,[37,38] Their unique gel-like properties make them an ideal material for application in pharmaceutical industry for drug release, in the food industry for flavor and nutrient delivery, and in biotechnology for tissue engineering.[39,40] Considering this, NO donor Nap-NO was incorporated into alginate beads for the controlled release of NO. The beads were characterized by SEM analysis, when exposed to LED light irradiation (420 nm, 3W), the alginate beads incorporated NO releasing molecule undergo a color change from colorless to a vibrant yellow that could be detected by naked-eye (Figure 5A). Further, non-emissive beads converted to brilliant green fluorescence (Figure 5B) after NO release.

Light-responsive behavior of alginate beads, offering a versatile platform for controlled NO delivery with a real-time visual monitoring by color and emission change (Scheme 3). This novel approach harnesses the unique properties of Nap-NO in polymer beads. Further, to confirm the NO release, alginate beads were immersed into the solution containing Griess reagent. A remarkable color change from colorless to pinkish appeared only when exposed to light. This result confirms the release of NO from the alginate polymer beads incorporated NO-releasing molecule (Figure 5C). Through Griess assay, it was estimated that the bead loaded with Nap-NO was able to release 6.63 μM amount of NO in water (Figure S18).

Further, time-dependent emission spectra of alginate beads were also recorded to monitor the changes in emission. For this experiment, a quartz cuvette was filled with alginate beads and then exposed to blue light (Figure S19). After the light exposure, an increase in intensity at 510–540 nm was observed, which is like the change observed in the solution system. This experiment further confirms the release of NO from the alginate gels.

Morphology and elemental mapping of the alginate beads were studied by SEM micrographs. As shown in Figure S20, alginate beads alone has well separated, homogeneous with smooth surface texture but after the incorporation Nap-NO, the surface of the beads become irregular and rough (Figure 6A). After irradiation with light, the morphology of the alginate beads became more irregular, which may be due to the release of NO (Figure 6D). Further, corresponding elemental analysis mapping (EDAX) for oxygen and nitrogen (Figures 6A–6D) atoms were performed to detect the NO release from hydrogel beads. As expected, a homogeneous distribution of nitrogen and oxygen was

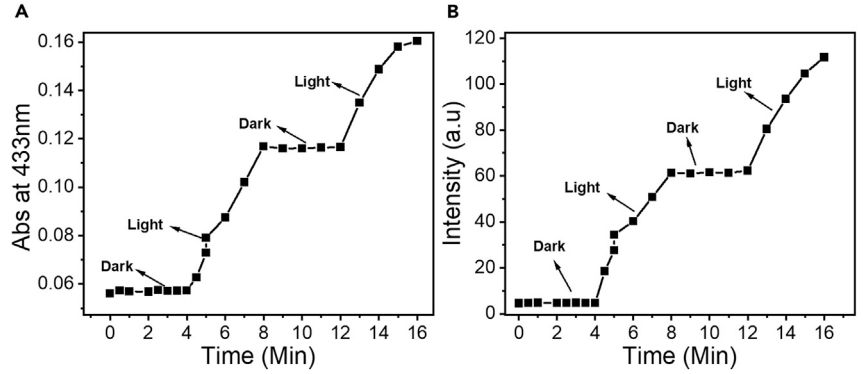

Figure 4. Stability of liposome in dark and light

(A and B) Time dependent change in (A) UV-vis absorption and (B) emission of **Nap-NO.Ves** under light and dark.

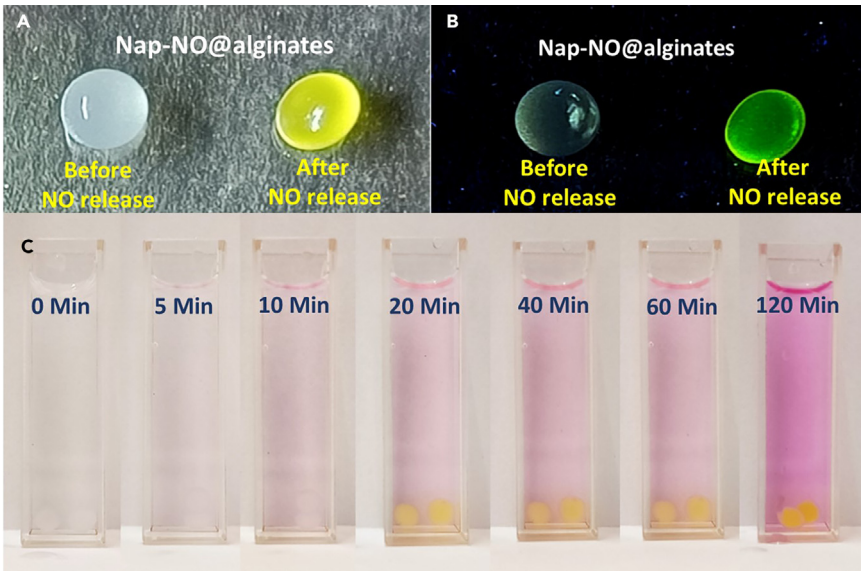

Figure 5. Changes in alginate beads before and after light irradiation

(A) Change in color of alginate beads containing Nap-NO before and after blue light irradiation (420 nm 3W) in daylight condition.

(B) Change in emission of alginate beads loaded with Nap-NO before and after NO release viewed under a 365 nm UV-lamp in a UV-chamber.

(C) Change in color of modified Griess reagent containing alginate bead loaded with Nap-NO upon blue light irradiation (420 nm 3W).

observed throughout the hydrogel surface before NO release (Figures 6B–6E). In contrast, the percentage of distribution is less after the NO release (Figures 6C–6F). The result of NO release from alginate beads is confirmed by IR analysis (Figure S21). IR stretching peak at 3,369 cm^{-1} responsible for -NH group was observed only after light irradiation, indicating the presence of N–H group and release of NO from Nap-NO. This result confirms the light-induced release of NO from the alginate-based hydrogels.

Bioimaging and cytotoxicity studies

To evaluate the safety profile of **Nap-NO.Ves** for potential phototherapeutic applications, cell viability assays using HCT cells were conducted across a concentration gradient spanning from 1.56 μM to 100 μM in triplicates. HCT cells, seeded for 24 h, were treated with NO-loaded vesicles under varying light irradiation conditions of the compound. No significant impact on cell viability and morphology was observed across the 100 μM–1.56 μM range before and after blue light irradiation of the compound. However, at 100 μM concentration, morphological changes and cell death occurred, while lower concentrations (<100 μM) exhibited over 90% viability. The cytotoxicity at higher concentrations without any light irradiation is probably ascribed to the casual release of NO by incidental lights in the lab. It suggests the biocompatibility of NO-loaded vesicles before and after irradiation.

Similarly, the safety profile of Nap-NO.Cho was also checked before and after irradiation with light (Figure S22). No noteworthy toxic profile was observed as that of **Nap-No.Ves**. This result suggests that **Nap-No.Ves** and Nap-NO.Cho are not toxic to the cell before and after the

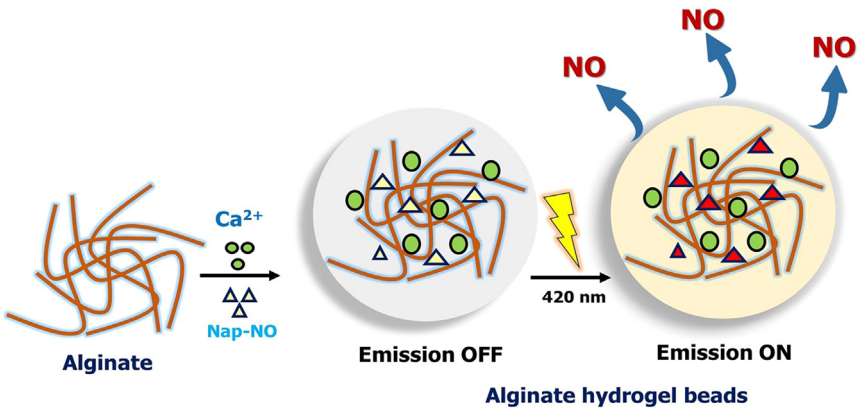

Scheme 3. Schematic representation for the preparation of Nap-NO incorporated alginate beads and their NO release

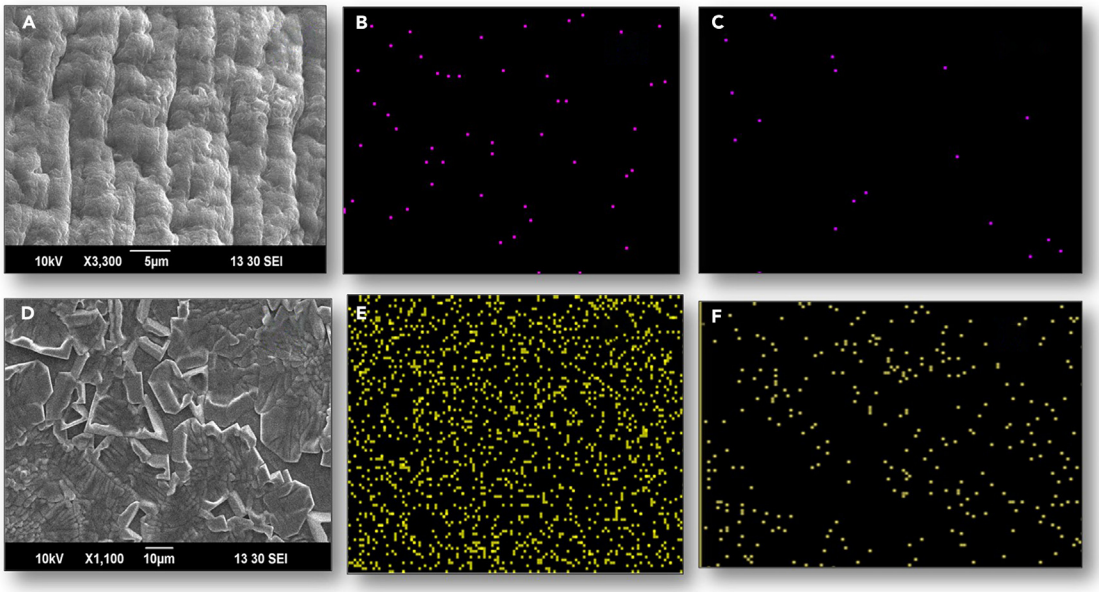

Figure 6. SEM and EDAX of alginate beads before and after light irradiation

(A–F) SEM images of Nap-NO incorporated alginate beads (A) before light irradiation and (D) after light irradiation. SEM-elemental analysis mapping (EDAX) (B for nitrogen; E for oxygen) before light irradiation and (C for nitrogen; F for oxygen) after light irradiation.

release of NO. These results confirm the safety of **Nap-NO.Ves** for utilization in cellular applications. Given the safety profile of **Nap-NO.Ves** in cellular applications, further research can now focus on its potential to promote nitric oxide (NO) release within biological cells. Following time-dependent cytotoxicity analysis revealed that light irradiation led to increased cell toxicity (Figure 7C). Figure 7D depicts that a 30-min irradiation period resulted in 50% cell death, with viability decreasing and changes in morphology progressively with shorter irradiation times. Cell viability assay with 420 nm (3W) was also checked to confirm the toxicity to the cells is due to the released NO and not due to light (Figure S23). This indicates that light-induced NO release is associated with a time-dependent decrease in cell viability. These findings underscore that **Nap-NO.Ves** has notable cancer cell membrane permeability and its potential as an effective NO delivery agent within cellular contexts.

Fluorescence imaging of HCT cells treated with NO-loaded vesicles revealed distinct observations in three channels: brightfield, green, and merged. Before irradiation, no green fluorescence was detected in the cells. However, after a 10-min irradiation period, a pronounced and sharp green fluorescence signal was observed. Figure 8 demonstrates that NO-loaded vesicles can serve as effective agents for bioimaging, as their fluorescence is activated in the presence of blue light, allowing for real-time visualization and detection within the cells.

In conclusion, our study represents a significant advancement in the field of NO delivery systems. We addressed the challenges associated with the limited bioavailability of NO by encapsulating NO-releasing compound (Nap-NO) within lipid-based vesicles composed of DOPC along with 30 mol % cholesterol. Our research demonstrated two crucial benefits of this incorporation strategy. First, it significantly improved the water solubility of the NO donor, overcoming a major limitation of many existing NO-releasing compounds. Second, it allowed for the regulation of NO-release kinetics, which holds promise for real-time applications. Through a comprehensive evaluation of NO-release kinetics using various assays and visualization techniques, we discovered a noteworthy difference between vesicles with DOPC and DOPC-cholesterol. The presence of cholesterol in the vesicular system led to a slower NO release rate and a significantly extended half-life compared to DOPC vesicles. This finding suggests that DOPC-cholesterol vesicles offer enhanced stability, making them a more attractive option for sustained NO delivery. Moreover, our study addressed the crucial aspect of biocompatibility by conducting cytotoxicity on HCT cell lines without using any organic co-solvent. Encouragingly, our NO-releasing probe exhibited negligible toxicity up to a concentration of 50 μM, reinforcing its potential for biomedical applications. Further NO-releasing vesicles also used for the bioimaging experiments within the HCT cell line. The cytotoxicity studies clearly illustrate the proficiency of NO releasing liposomes in killing cancer cells upon NO delivery, thereby unveiling promising avenues for precise NO administration within cellular environments. Within a biocompatible and water-soluble framework of liposomes, the present findings hold promise for the development of novel therapeutic agents and diagnostic tools that harness the unique properties of NO in a controlled and sustained manner upon light irradiation that can be easily monitored by color and emission changes. Overall, this study offers a safer and more biocompatible approach using liposomal delivery of NO and modulation of NO release kinetics by lipid fluidity.

Limitations of the study

While the present NO-releasing system shows toxicity to cancer cells, more detailed investigations and *in vivo* studies are required to understand the therapeutic potential. In this report, the photo-controlled release of NO was achieved by using blue light (420 nm); however, it would

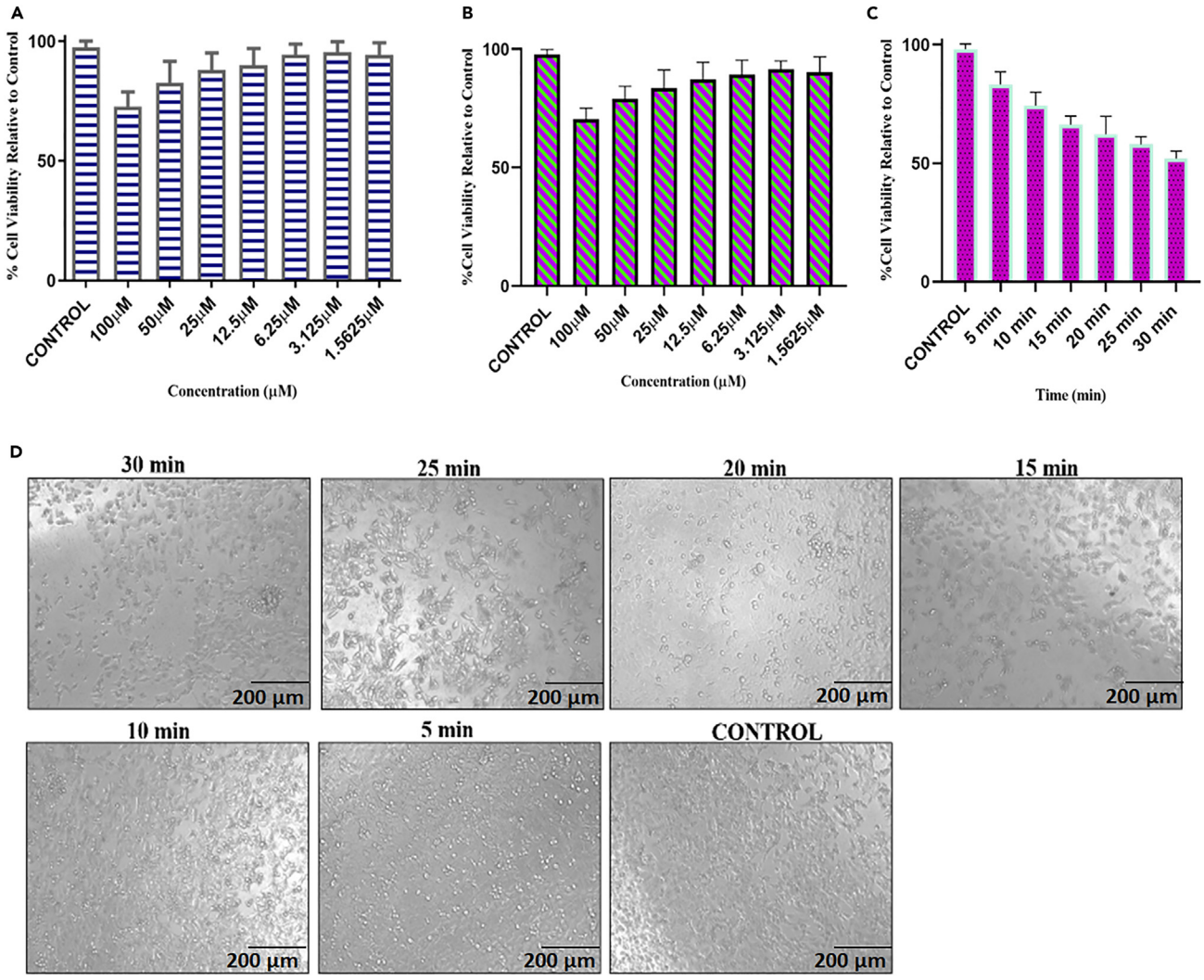

Figure 7. Cytotoxicity of Nap-No.Ves on HCT cell line

(A and B) Cytotoxicity of **Nap-NO.Ves** on HCT cell line (A) before irradiation and (B) after irradiation.

(C) Time-dependent cytotoxicity studies after irradiation within the cells followed by the treatment of **Nap-NO.Ves** (50 μM), the values are the average of three independent experiments.

(D) The microscope images of cells upon irradiation with light (420 nm 3W) on different time interval. Data are represented as means + EESE of multiple experiments (n = 3).

be better to achieve the NO release using NIR (near-infrared) light, which would be more advantageous for pharmacotherapy. Also, the present system is not comparable with the established NO-releasing drugs like isosorbide dinitrate and isosorbide mononitrate, because the NO-releasing mechanism of these drugs are different; the present system releases NO in the presence of light whereas the established drugs does not need any light. Also, light-induced NO-releasing donors need to be stored in under dark to avoid the casual release of NO by incidental lights in the storage area.

STAR★METHODS

Detailed methods are provided in the online version of this paper and include the following:

- KEY RESOURCES TABLE
- RESOURCE AVAILABILITY
  - Lead contact
  - Materials availability

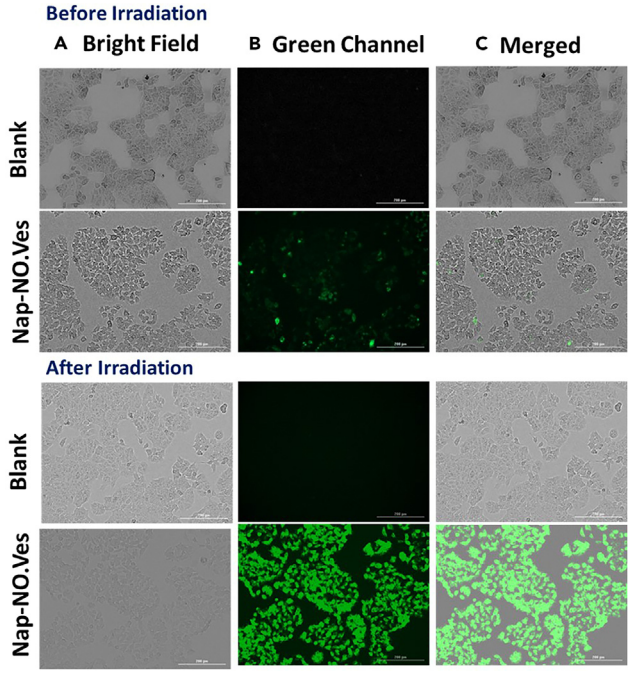

Figure 8. Imaging of Nap-No.Ves on HCT cell line

Fluorescence laser scanning microscope images of HCT cell lines. (A) Brightfield, (B) green channel, and (C) merged image of cells incubated with **Nap-NO.Ves** before and after blue light (420 nm, 3W) irradiation at 37°C.

SUPPLEMENTAL INFORMATION

Supplemental information can be found online at https://doi.org/10.1016/j.isci.2024.110230.

ACKNOWLEDGMENTS

D.A.J. acknowledges to Science and Engineering Research Board, New Delhi, Core Research Grant no CRG/2022/004990, and Haryana State Council of Science Innovation and Technology (HSCSIT), Haryana and CSIR-India for the CSIR-EMR(II) grant no 01/3127/23/EMR-II. V.K. thanks MHRD for financial help.

AUTHOR CONTRIBUTIONS

Conceptualization, D.A.J and V.K.; methodology, V.K., Kanika, and N.S.; investigation, V.K., Kanika, N. S., R.S., and R.K.; writing – original draft, D.A.J., V.K., Kanika, and R.K.; writing – review and editing, D.A.J., R. K., and V.K.; funding ccquisition, D.A.J.; resources, D.A.J. and R.K.; supervision, D.A.J. and R.K.

DECLARATION OF INTERESTS

The authors declare no competing interests.

Received: November 30, 2023
Revised: March 2, 2024
Accepted: June 6, 2024
Published: June 9, 2024

REFERENCES

1. Paul, S., Pan, S., Mukherjee, A., and De, P. (2021). Nitric Oxide Releasing Delivery Platforms: Design, Detection, Biomedical Applications, and Future Possibilities. Mol. Pharm. *18*, 3181–3205. https://doi.org/10.1021/acs.molpharmaceut.1c00486.
2. Pieretti, J.C., Pelegrino, M.T., Silveira, N.M., Rodrigues, M.G., and Seabra, A.B. (2023). State-of-the-Art and Perspectives for Nanomaterials Combined with Nitric Oxide Donors: From Biomedical to Agricultural Applications. ACS Appl. Nano Mater. *18*, 3181–3205. https://doi.org/10.1021/acsanm.3c03482.
3. van der Vlies, A.J., Yamane, S., and Hasegawa, U. (2024). Recent advance in self-assembled polymeric nanomedicines for gaseous signaling molecule delivery. Wiley Interdiscip. Rev. Nanomed. Nanobiotechnol. *16*, e1934. https://doi.org/10.1002/wnan.1934.
4. Wang, Z., Jin, A., Yang, Z., and Huang, W. (2023). Advanced Nitric Oxide Generating Nanomedicine for Therapeutic Applications. ACS Nano *17*, 8935–8965. https://doi.org/10.1021/acsnano.3c02303.
5. Gao, D., Asghar, S., Hu, R., Chen, S., Niu, R., Liu, J., Chen, Z., and Xiao, Y. (2023). Recent advances in diverse nanosystems for nitric oxide delivery in cancer therapy. Acta Pharm. Sin. B *13*, 1498–1521. https://doi.org/10.1016/j.apsb.2022.11.016.
6. Kabirian, F., Baatsen, P., Smet, M., Shavandi, A., Mela, P., and Heying, R. (2023). Carbon nanotubes as a nitric oxide nano-reservoir improved the controlled release profile in 3D printed biodegradable vascular grafts. Sci. Rep. *13*, 4662. https://doi.org/10.1038/s41598-023-31619-3.
7. Saraiva, J., Marotta-Oliveira, S.S., Cicillini, S.A., Eloy, J.d.O., and Marchetti, J.M. (2011). Nanocarriers for nitric oxide delivery. J. Drug Deliv. *2011*, 936438. https://doi.org/10.1155/2011/936438.
8. Naghavi, N., de Mel, A., Alavijeh, O.S., Cousins, B.G., and Seifalian, A.M. (2013). Nitric Oxide Donors for Cardiovascular Implant Applications. Small *9*, 22–35. https://doi.org/10.1002/smll.201200458.
9. Chen, L., Tan, G., Chen, H., and Liu, J. (2016). Nitric oxide-donor drugs and prostate cancer: an update. Zhongliu Fangzhi Yanjiu *43*, 162–166. https://doi.org/10.3971/j.issn.1000-8578.2016.02.014.
10. Li, B., Ming, Y., Liu, Y., Xing, H., Fu, R., Li, Z., Ni, R., Li, L., Duan, D., Xu, J., et al. (2020). Recent developments in pharmacological effect, mechanism and application prospect of diazeniumdiolates. Front. Pharmacol. *11*, 00923. https://doi.org/10.3389/fphar.2020.00923.
11. Zhou, X., Zhang, J., Feng, G., Shen, J., Kong, D., and Zhao, Q. (2016). Nitric Oxide-Releasing Biomaterials for Biomedical Applications. Curr. Med. Chem. *23*, 2579–2601. https://doi.org/10.2174/0929867323666160729104647.
12. Xiang, H.-j., Liu, J.-g., and Zhao, Y. (2017). Recent research advancements in NO-releasing nanomaterials. Wuli Huaxue Xuebao *33*, 903–917. https://doi.org/10.3866/pku.whxb201702091.
13. Sharma, R., Joubert, J., and Malan, S.F. (2018). Recent Developments in Drug Design of NO-donor Hybrid Compounds. Mini Rev. Med. Chem. *18*, 1175–1198. https://doi.org/10.2174/1389557518666180416150005.
14. Cheng, J., He, K., Shen, Z., Zhang, G., Yu, Y., and Hu, J. (2019). Nitric oxide (NO)-releasing macromolecules: rational design and biomedical applications. Front. Chem. *7*, 530. https://doi.org/10.3389/fchem.2019.00530.
15. Wu, M., Lu, Z., Wu, K., Nam, C., Zhang, L., and Guo, J. (2021). Recent advances in the development of nitric oxide-releasing biomaterials and their application potentials in chronic wound healing. J. Mater. Chem. B *9*, 7063–7075. https://doi.org/10.1039/d1tb00847a.
16. Rose, M.J., and Mascharak, P.K. (2008). Photoactive ruthenium nitrosyls: Effects of light and potential application as NO donors. Coord. Chem. Rev. *252*, 2093–2114. https://doi.org/10.1016/j.ccr.2007.11.011.
17. Navale, G.R., Singh, S., and Ghosh, K. (2023). NO donors as the wonder molecules with therapeutic potential: Recent trends and future perspectives. Coord. Chem. Rev. *481*, 215052. https://doi.org/10.1016/j.ccr.2023.215052.
18. deBoer, T.R., and Mascharak, P.K. (2015). Chapter Three - Recent Progress in Photoinduced NO Delivery With Designed Ruthenium Nitrosyl Complexes. In Advances in Inorganic Chemistry, R. van Eldik and J.A. Olabe, eds. (Academic Press), pp. 145–170. https://doi.org/10.1016/bs.adioch.2014.11.002.
19. Juarez-Martinez, Y., Labra-Vázquez, P., Enríquez-Cabrera, A., Leon-Rojas, A.F., Martínez-Bourget, D., Lacroix, P.G., Tassé, M., Mallet-Ladeira, S., Farfán, N., Santillan, R., et al. (2022). Bimetallic Ruthenium Nitrosyl Complexes with Enhanced Two-Photon Absorption Properties for Nitric Oxide Delivery. Chem. Eur J. *28*, e202201692. https://doi.org/10.1002/chem.202201692.
20. Jiang, Y., Huang, S., Liu, M., Weng, J., You, W., Du, X., Zhang, H., Qian, J., and Sun, H. (2024). Mitochondria-targeted NO donor enables synergistic NO and photodynamic therapies for effective inhibition of cancer cell proliferation and migration. Dyes Pigments *221*, 111810. https://doi.org/10.1016/j.dyepig.2023.111810.
21. Zhang, Z., Wu, J., Shang, Z., Wang, C., Cheng, J., Qian, X., Xiao, Y., Xu, Z., and Yang, Y. (2016). Photocalibrated NO Release from N-Nitrosated Napthalimides upon One-Photon or Two-Photon Irradiation. Anal. Chem. *88*, 7274–7280. https://doi.org/10.1021/acs.analchem.6b01603.
22. Zhang, S., Wang, Q., Yang, J., Yang, X.-F., Li, Z., and Li, H. (2019). A photocalibrated NO donor based on N-nitrosorhodamine 6G upon UV irradiation. Chin. Chem. Lett. *30*, 454–456. https://doi.org/10.1016/j.cclet.2018.03.011.
23. Dong, H.-Q., Wei, T.-B., Ma, X.-Q., Yang, Q.-Y., Zhang, Y.-F., Sun, Y.-J., Shi, B.-B., Yao, H., Zhang, Y.-M., and Lin, Q. (2020). 1,8-Naphthalimide-based fluorescent chemosensors: recent advances and perspectives. J. Mater. Chem. C *8*, 13501–13529. https://doi.org/10.1039/D0TC03681A.
24. Sharma, N., Arjunan, P., Marepally, S., Jain, N., Naziruddin, A.R., Ghosh, A., Mariappan, C.R., and Jose, D.A. (2022). Photo controlled release of nitric oxide (NO) from amphiphilic and nanoscale vesicles based ruthenium nitrosyl complex: NO release and cytotoxicity studies. J. Photochem. Photobiol., A *425*, 113703. https://doi.org/10.1016/j.jphotochem.2021.113703.
25. Sharma, N., Jose, D.A., Jain, N., Parmar, S., Srivastav, A., Chawla, J., Naziruddin, A.R., and Mariappan, C.R. (2022). Regulation of Nitric Oxide (NO) Release by Membrane Fluidity in Ruthenium Nitrosyl Complex-Embedded Phospholipid Vesicles. Langmuir *38*, 13602–13612. https://doi.org/10.1021/acs.langmuir.2c02457.
26. Sharma, N., Kumar, V., and Jose, D.A. (2023). A ruthenium nitrosyl complex-based highly selective colorimetric sensor for biological H2S and H2S–NO cross-talk regulated release of NO. Dalton Trans. *52*, 675–682. https://doi.org/10.1039/D2DT03108F.
27. Tahara, Y., Yoshikawa, T., Sato, H., Mori, Y., Zahangir, M.H., Kishimura, A., Mori, T., and Katayama, Y. (2017). Encapsulation of a nitric oxide donor into a liposome to boost the enhanced permeation and retention (EPR) effect. MedChemComm *8*, 415–421. https://doi.org/10.1039/C6MD00614K.
28. Liu, S., Li, G., and Ma, D. (2022). Controllable Nitric Oxide-Delivering Platforms for Biomedical Applications. Adv. Ther. *5*, 2100227. https://doi.org/10.1002/adtp.202100227.
29. Coneski, P.N., and Schoenfisch, M.H. (2012). Nitric oxide release: Part III. Measurement and reporting. Chem. Soc. Rev. *41*, 3753–3758. https://doi.org/10.1039/C2CS15271A.
30. Mirzavi, F., Barati, M., Soleimani, A., Vakili-Ghartavol, R., Jaafari, M.R., and Soukhtanloo, M. (2021). A review on liposome-based therapeutic approaches against malignant melanoma. Int. J. Pharm. *599*, 120413. https://doi.org/10.1016/j.ijpharm.2021.120413.
31. Gadiyaram, S., Sharma, N., Enoch, I.V.M.V., and Jose, D.A. (2022). Multi analyte sensing of amphiphilic tridentate bis(benzimidazolyl) pyridine incorporated in liposomes and potential application in enzyme assay. Anal.

Methods *14*, 2357–2367. https://doi.org/10.1039/D2AY00486K.

32. Kumar, V., Sakla, R., Sharma, N., Jose, D.A., Kanika, and Khan, R. (2023). Liposome Based Near-Infrared Sensors for the Selective Detection of Hydrogen Sulfide. ChemPlusChem *88*, e202300243. https://doi.org/10.1002/cplu.202300243.
33. Sakla, R., and Jose, D.A. (2018). Vesicles Functionalized with a CO-Releasing Molecule for Light-Induced CO Delivery. ACS Appl. Mater. Interfaces *10*, 14214–14220. https://doi.org/10.1021/acsami.8b03310.
34. Zhang, Y., Li, Q., Dong, M., and Han, X. (2020). Effect of cholesterol on the fluidity of supported lipid bilayers. Colloids Surf. B Biointerfaces *196*, 111353. https://doi.org/10.1016/j.colsurfb.2020.111353.
35. Zhang, X., Barraza, K.M., and Beauchamp, J.L. (2018). Cholesterol provides nonsacrificial protection of membrane lipids from chemical damage at air–water interface. Proc. Natl. Acad. Sci. USA *115*, 3255–3260. https://doi.org/10.1073/pnas.1722323115.
36. Banerjee, S., Bhuyan, M., and König, B. (2013). Tb(iii) functionalized vesicles for phosphate sensing: membrane fluidity controls the sensitivity. Chem. Commun. *49*, 5681–5683. https://doi.org/10.1039/C3CC42132E.
37. Bright, L.M.E., Wu, Y., Brisbois, E.J., and Handa, H. (2023). Advances in nitric oxide-releasing hydrogels for biomedical applications. Curr. Opin. Colloid Interface Sci. *66*, 101704. https://doi.org/10.1016/j.cocis.2023.101704.
38. Urzedo, A.L., Gonçalves, M.C., Nascimento, M.H.M., Lombello, C.B., Nakazato, G., and Seabra, A.B. (2020). Multifunctional alginate nanoparticles containing nitric oxide donor and silver nanoparticles for biomedical applications. Mater. Sci. Eng. C *112*, 110933. https://doi.org/10.1016/j.msec.2020.110933.
39. Zheng, G., Li, R., Wu, P., Zhang, L., Qin, Y., Wan, S., Pei, J., Yu, P., Fu, K., Meyerhoff, M.E., et al. (2023). Controllable release of nitric oxide from an injectable alginate hydrogel. Int. J. Biol. Macromol. *252*, 126371. https://doi.org/10.1016/j.ijbiomac.2023.126371.
40. Estes Bright, L.M., Griffin, L., Mondal, A., Hopkins, S., Ozkan, E., and Handa, H. (2022). Biomimetic gasotransmitter-releasing alginate beads for biocompatible antimicrobial therapy. J. Colloid Interface Sci. *628*, 911–921. https://doi.org/10.1016/j.jcis.2022.08.113.
41. Sarkar, S., Kumar, R., and Matson, J.B. (2024). Hydrogels for Gasotransmitter Delivery: Nitric Oxide, Carbon Monoxide, and Hydrogen Sulfide. Macromol. Biosci. *24*, 2300138. https://doi.org/10.1002/mabi.202300138.
42. Sakla, R., and Amilan Jose, D. (2021). New fluorinated manganese carbonyl complexes for light-controlled carbon monoxide (CO) release and the use of benchtop ^{19}F-NMR spectroscopy. Inorg. Chim. Acta. *516*, 120134. https://doi.org/10.1016/j.ica.2020.120134.
43. Balzani, V., Ceroni, P., and Juris, A. (2014). Photochemistry and Photophysics: Concepts, Research, Applications (John Wiley & Sons).

STAR★METHODS

KEY RESOURCES TABLE

REAGENT or RESOURCE	SOURCE	IDENTIFIER
Chemicals, peptides, and recombinant proteins		
Ethanol	Local supplier	CAS: 64-17-5
2-methoxy ethanol	Sigma Aldrich	CAS: 109-86-4
Tetrahydrofuran	Loba Chemie	CAS: 109-99-9
Glacial acetic acid	Loba Chemie	CAS: 64-19-7
Sodium nitrite	Sigma Aldrich	CAS: 7632-00-00
Ethyl acetate	Finar	CAS: 141-78-6
Hexane	Finar	CAS: 110-54-3
4-bromo-1,8 napthalic anhydride	Sigma Aldrich	CAS: 81-86-7
Octadecylamine	Sigma Aldrich	CAS: 124-30-1
methylamine hydrochloride	Sigma Aldrich	CAS: 593-51-1
sodium bicarbonate	Loba Chemie	CAS: 144-55-8
Dichloromethane	Finar	CAS: 75-09-2
1,2-Dioleoyl-*sn*-glycero-3-phosphocholine (DOPC)	Sigma Aldrich	CAS: 4235-95-4
HEPES	Sigma Aldrich	CAS: 7365-45-9
Cholesterol	Sigma Aldrich	CAS: 57-88-5
DMSO	Loba Chemie	CAS: 67-68-5
Modified Griess reagent	Sigma Aldrich	CAS: 1465-25-4
Sodium alginate	Loba Chemie	CAS: 9005-38-3
Calcium chloride	Loba Chemie	CAS: 10043-52-4
Methanol	Loba Chemie	CAS: 67-56-1
silica-gel (mesh size 100–200)	Loba Chemie	CAS: 112926-00-8
Fetal Bovine Serum (FBS)	Sigma Aldrich	Product no: 12003C
Streptomycin	Sigma Aldrich	CAS: 3810-74-0
MTT (3-[4,5-dimethylthiazol-2-yl]-2, 5-diphenyltetrazolium bromide	Sigma Aldrich	CAS: 298-93-1
Trypsin	Sigma Aldrich	CAS: 9002-07-7
Dulbecco's Modified Eagle Medium (DMEM)	Sigma Aldrich	D6429
Experimental models: Cell lines		
Human colon cancer cell line (HCT)	National Center for Cell Science (NCCS) in Pune, India	
Software and algorithms		
ChemDraw Ultra 12.0	PerkinElmer	https://www.perkinelmer.com/category/chemdraw
MestReNova	Mestrelab Research chemistry software solutions.	https://mestrelab.com/
OriginPro 8.5	OriginLab	https://www.originlab.com/

RESOURCE AVAILABILITY

Lead contact

Further information and requests for resources and reagents should be directed to and will be fulfilled by the lead contact, D. Amilan jose (amilanjosenit@nitkkr.ac.in).

Materials availability

This study did not generate new unique reagents.

Data and code availability

- All data reported in this paper will be shared by the lead contact upon request.
- This paper does not report the original code.
- Any additional information required to reanalyse the data reported in this work paper is available from the lead contact upon request.

EXPERIMENTAL MODEL AND STUDY PARTICIPANT DETAILS

Cell culture

Human colon cancer cell line (HCT) were supplied by the National Center for Cell Science in Pune, India. The cells at passages 3- S were cultured in DMEM media with 10% Fetal Bovine Serum (FBS), and 100 μg/mL, streptomycin at a standard condition of 37°C temperature within a 5% CO_2 incubation environment. All the cells were authenticated by observing their morphology under the microscope carefully and cultured in a strict mycoplasma-free conditions.

METHOD DETAILS

All chemicals and solvents are commercially available and were used as it is. 2-methoxy ethanol, Sodium nitrite, 4-bromo-1,8 napthalic anhydride, octadecylamine, methylamine hydrochloride, 1,2-Dioleoyl-*sn*-glycero-3-phosphocholine (DOPC), HEPES, Cholesterol, Modified Griess reagent, Fetal Bovine Serum (FBS), Streptomycin, MTT (3-[4,5-dimethylthiazol-2-yl]-2,5-diphenyltetrazolium bromide, Dulbecco's Modified Eagle Medium (DMEM) and Trypsin were purchased from Sigma-Aldrich. Tetrahydrofuran, Glacial acetic acid, sodium bicarbonate, DMSO, Sodium alginate, Calcium chloride, Methanol and silica-gel (mesh size 100–200) purchased from Loba-Chemie. Ethyl acetate, Hexane, Dichloromethane purchased from Finar Chemical limited. UV-Vis absorption spectra were recorded using the Cary Eclipse UV-Vis spectrophotometer from Agilent Technologies. Emission measurements were conducted using the Cary Eclipse fluorescence spectrophotometer. For ^{1}H-NMR and ^{13}C-NMR measurements, the Bruker Avance II 400 MHz NMR Spectrometer was employed. The Shimadzu IR Affinity spectrophotometer, utilizing KBr as a standard, was used for FT-IR spectrum analysis.

Synthesis of compounds

Synthesis of 6-bromo-3-octadecyl-1H-benzoisoquinoline-1,3(2H)-dione (Nap-Br)

1g (1.8 mmol) of 4-bromo-1,8-naphthalic anhydride and 1.23g (1.8 mmol) of 1-Octadecanamine was dissolved in 100 mL dry ethanol and refluxed of 12 h. The reaction mixture was permitted to gradually attain room temperature. The resulting precipitate was isolated through filtration. Subsequent purification of the compound was performed by using silica gel column chromatography utilizing a mixture of ethyl acetate and hexane as eluent to provide yield 1.65g (95%) of product. ^{1}H NMR (500 MHz, $CDCl_3$) δ 8.57 (dd, *J* = 7.3, 1.1 Hz, 1H), 8.47 (dd, *J* = 8.5, 1.1 Hz, 1H), 8.32 (d, *J* = 7.8 Hz, 1H), 7.95 (d, *J* = 7.9 Hz, 1H), 7.76 (dd, *J* = 8.5, 7.3 Hz, 1H), 4.10–4.06 (m, 2H), 1.65 (t, *J* = 7.6 Hz, 2H), 1.17 (d, *J* = 2.5 Hz, 30H), 0.80 (t, *J* = 7.0 Hz, 3H). ^{13}C NMR (126 MHz, $CDCl_3$) δ 163.56, 163.54, 133.14, 131.96, 131.15, 131.06, 130.59, 130.12, 128.97, 128.04, 123.17, 122.31, 40.64, 31.93, 29.70, 29.67, 29.65, 29.61, 29.55, 29.36, 28.09, 27.13, 22.69. ESI-MS m/z: calculated for $[C_{30}H_{42}BrNO_2]^+$: 528.58, found: $[M]^+$:528.2080, $[M + H]^+$:529.2113, $[M+2H]^+$:530.2055.

Synthesis of 6-bromo-3-octadecyl-1H-benzoisoquinoline-1,3(2H)-dione (Nap-NH)

In a 100 mL RB flask, 1g (1.89 mmol) of 6-Bromo-3-octadecyl-1H-benzoisoquinoline-1,3(2H)-dione **(Nap-Br)**, 319 mg (4.7 mmol) of methylamine hydrochloride, 397 mg (4.7 mmol) of sodium bicarbonate, was dissolved in 2-methoxyethanol (50 mL). The mixture was heated to 110°C with constant stirring for 8 h, then it was allowed to cool at room temperature and evaporated under reduced pressure. The precipitate was extracted by using dichloromethane and the organic layer was evaporated under reduced pressure. The crude product was then further purified using silica gel column chromatography using CH_2Cl_2/MeOH (100:2 v/v) as the eluent yielding 700 mg of **Nap-NH** (Yield = 77% yield). ^{1}H NMR (500 MHz, $CDCl_3$) δ 8.57 (d, *J* = 0.6 Hz, 1H), 8.51 (dd, *J* = 23.5, 8.3 Hz, 1H), 8.07 (d, *J* = 7.9 Hz, 1H), 7.74–7.54 (m, 1H), 6.71 (d, *J* = 8.4 Hz, 1H), 5.40 (d, *J* = 4.6 Hz, 1H(NH)), 4.17–4.12 (m, 2H), 3.14 (d, *J* = 4.8 Hz, 3H), 1.72 (t, *J* = 7.6 Hz, 2H), 1.44–1.38 (m, 2H), 1.24 (d, *J* = 5.0 Hz, 28H), 0.87 (t, *J* = 6.9 Hz, 3H). ^{13}C NMR (126 MHz, $CDCl_3$) δ 165.18, 164.69, 150.67, 134.94, 131.55, 130.20, 126.17, 125.25, 123.81, 120.77, 111.15, 104.47, 40.78, 32.43, 31.06, 30.21, 30.16, 30.14, 30.09, 29.95, 29.87, 28.74, 27.73, 23.20, 14.62. ESI -MS m/z: calculated for $[C_{31}H_{46}N_2O_2]^+$: 478.36, found: $[M + H]^+$:479.3296, $[M+2H]^+$:480.3306.

Synthesis of Nap-NO

330 mg (0.69 mmol) of 6-Metylamino-3-octadecyl-1H-benzoisoquinoline-1,3(2H)-dione **(Nap-NH)** was dissolved in a mixture of acetic acid and THF (1:1 v/v, 20 mL) and then cooled to 0°C under ice. Gradually, sodium nitrite (476.3 mg, 6.9 mmol) was added to the solution slowly with continuous stirring. Once the addition was complete, the reaction mixture was allowed to gradually reach room temperature and was stirred for 2 h. The reaction mixture was neutralized with concentrated $NaHCO_3$ and extracted with CH_2Cl_2. The organic layer was evaporated under reduced pressure to obtain the solid product. Flash column chromatography was performed using silica gel under the dark using CH_2Cl_2 and MeOH (100:1 v/v) as the eluent to yield 200 mg of the final product. The desired compound was obtained as a crystalline light yellow solid. Yield 57%. ^{1}H NMR (500 MHz, $CDCl_3$) δ 8.58 (d, *J* = 7.2 Hz, 1H), 8.49 (d, *J* = 8.4 Hz, 1H), 8.07 (d, *J* = 8.2 Hz, 1H), 7.64–7.59 (m, 1H), 6.71 (d, *J* = 8.4 Hz, 1H), 4.17–4.13 (m, 2H), 3.14 (s, 3H), 1.72 (t, *J* = 7.6 Hz, 2H), 1.40 (dd, *J* = 15.0, 7.5 Hz, 2H), 1.25 (s, 28H), 0.88 (t, *J* = 6.9 Hz, 3H). ^{13}C NMR (101

MHz, $CDCl_3$) δ 162.79, 162.20, 142.77, 130.94, 130.00, 128.46, 127.76, 127.13, 125.94, 122.16, 121.57, 95.06, 39.67, 35.13, 30.89, 28.67, 28.63, 28.58, 28.53, 28.37, 28.34, 27.12, 26.10, 21.67, 13.05. ESI-MS m/z: calculated for $[C_{31}H_{45}N_3O_3]^+$: 507.3461, found: $[M]^+$:507.9194, $[M + H]^+$:508.9163.

General procedure for the preparation of liposomes

The thin film hydration technique was employed for the preparation of liposomes.[24] Accordingly, a solution containing 1 mg of the compound dissolved in chloroform, and lipid (1 mM) DOPC, was prepared with the NO-donor (**Nap-NO.Ves**) to phospholipid molar ratio is (10:1). This mixture was then transferred to a small round-bottom flask. By gradually evaporating under vacuum conditions, a thin layer of lipid cake was formed. Subsequently, 5 mL of HEPES buffer (10 mM, pH = 7.4) was introduced, followed by heating the mixture to 70°C for 30 min while subjecting it to bathe sonication. This controlled process led to the formation of multilamellar vesicles within the fluid. To generate a solution of unilamellar vesicles, the aforementioned solution was repetitively passed through a polycarbonate membrane with 100 nm pore size. This solution was then stored overnight to facilitate further investigations. Two different types of liposomes were formed with different combinations of cholesterol and lipid, one with only DOPC (**Nap-NO.Ves**) and the other one with 30% mol of cholesterol and DOPC (**Nap-NO.Cho**).

Nitric oxide release studies of Nap-NO by UV-Visible and emission spectroscopy

UV-Vis absorption spectroscopy and emission spectroscopy was used to investigate the NO release of Nap-NO. UV-Vis spectra and emission spectra were recorded with 2 mL (40 μM) of Nap-NO in a DMSO/H_2O mixture. Time-dependent absorption and emission spectrum was recorded in a quartz cuvette with a path length of 1 cm, and subjected to light irradiation at a wavelength of 420 nm (3W). The light source was positioned 1 cm away from the quartz cuvette. The change in absorbance at 433 nm and the change in emission 522 nm was monitored to quantify the NO release.

Nitric oxide release studies of Nap-NO.Ves and Nap-NO.Cho by UV-Visible and emission spectroscopy

UV-Vis and emission spectra were recorded for a 2 mL solution of **Nap-NO.Ves** (16 μM) or Nap-NO.Cho (16 μM) in HEPES Buffer (10 mM). The solution was placed in a quartz cuvette with a path length of 1 cm, and subjected to light irradiation at a wavelength of 420 nm (3W). The light source was positioned 1 cm away from the quartz cuvette, and the changes in emission and absorbance were monitored.

Griess assay with Nap-NO.Ves

A stock greiss reagent solution (100 mg) was prepared by dissolving it in 2.5 mL of HEPES buffer (10 mM).[24,25,41] Subsequently, 200 μL of this stock Griess reagent solution was added into 2 mL solution of HEPES buffer containing **Nap-NO.Ves** (16 μM). To monitor the progression of the reaction, UV-Vis spectra was recorded at different time intervals following exposure to irradiation with blue light (420 nm, 3W) positioned 1 cm away from the quartz cuvette. The observed increase in absorbance at 540 nm served as a reliable indicator for the formation of an azo dye and NO release from the **Nap-NO.Ves**.

Preparation of alginate beads incorporated with Nap-NO

A 50 mL aqueous solution of sodium alginate, with a concentration ranging from 2% to 2.5% w/v, was meticulously introduced drop by drop from a glass syringe into the solution of 100 mL $CaCl_2$ solution concentrations varying from 1% to 3% w/v. For loading of NO donor, 10 mg of Nap-NO was dissolved in DMSO and then added to the sodium alginate solution. Subsequently, alginate beads were prepared using a similar method as described above for the preparation of blank beads. The NO donor loaded beads were then exposed to blue light for half an hour, and the change in emission and color were monitored to know the NO release in the gel state. The emission spectra of these beads were also recorded at regular intervals to monitor the changes in emission. To do this, a quartz cuvette was filled with alginate beads and then exposed to blue light. After the light exposure, an increase in intensity at 510–530 nm was observed, indicating the release of NO.

Cancer cell cytotoxicity and bio-imaging studies

HCT-116 human colorectal cancer cells were cultured in DMEM growth media supplemented with 10% FBS and streptomycin in a CO_2 incubator under standard conditions. Upon reaching the log phase of growth, cells were harvested, and the medium was regularly refreshed. Subsequently, 96-well plates were seeded with 5,000 HCT cells and allowed 24 h for confluence. **Nap-NO.Ves** before and after irradiation with blue light outside *in vitro* conditions were added to the cells, so that NO can be released outside only. These vesicles were administered in descending concentrations in the media for a 24-h treatment period. After the treatment, media was removed and cells were rinsed with PBS. Following treatment, 10 μL of a 5-mg/mL MTT solution was added to each well, and the plate was incubated for 2 h. After removing the culture media, formazan crystals were dissolved using 100 μL of dimethyl sulfoxide (DMSO), and cell viability was determined by measuring absorbance at 570 nm, indicating the percentage of viability relative to the control. Further, time-dependent study was conducted by irradiating the vesicle directly in the cells after giving the treatment. A subsequent time-dependent cell viability study involved seeding cells for 24 h, treating with a fixed concentration of 50 μM of Nap-NO loaded into vesicles, and subjecting them to blue light irradiation (420 nm, 3W) at different time points. The MTT method was then employed to assess cell viability post-irradiation. All the experiments were performed in triplicates. Fluorescence imaging was done according to the previously reported method. After confluency the treatment was given and irradiated for 10 min, later imaging was done on cytation instrument.

Transmission electron microscopy and SEM studies

Field Emission Scanning Electron Microscopy was used for the examination of liposome shape and size. Liposomes, following dilution with ultrapure water, were applied to a silicon wafer and subjected to gold sputter-coating. The examination was conducted using the JSM IT300LV instrument from JEOL. This high-resolution modality provided exhaustive insights into liposomal topography, furnishing detailed information concerning size distribution and morphological attributes. The examination of liposomal nanostructures was conducted via TEM utilizing the JEOL JEM-2100 instrument manufactured by JEOL, Japan. To optimize imaging conditions, the liposomal solution underwent dilution with distilled water and was subsequently deposited onto a 300-mesh carbon-coated copper grid. Subsequent observation using TEM facilitated high-resolution imaging, enabling the elucidation of intricate details pertaining to liposomal nanostructures.

Calculation of photon flux

The blue LED light source's photon flux (q_{in}) was measured using a previously described approach.[42] To achieve this, solutions containing 1,10-phenanthroline (X), potassium ferrioxalate trihydrate (W), and sodium acetate buffer (Y) in concentrations of 6 mM each were made. A 3 mL solution of W was exposed to photodecomposition for various times in a quartz cuvette by being positioned 3 cm from an LED light source. After that, 1 mL of the photodecomposed sample was incubated with 1 mL of solution X, 0.5 mL of solution Y, and 7.5 mL of deionized water for 1 h in complete darkness. The same procedure was used to incubate a control solution, which included 1 mL of solution W but was not exposed to irradiation. Both the irradiation and control samples' absorbance at 510 nm was measured after the incubation time. With a molar extinction coefficient ε of 11100 $M^{-1}cm^{-1}$, Lambert Beer's law was then used to determine the concentration of $[Fe(phen)_3]^{2+}$.

The equation given below was used to calculate how many Fe^{2+} ions were produced during photodecomposition:

$$nFe^{2+} = \frac{V_1 V_3 \Delta A_{510}}{10^3 \times l\varepsilon V_2}$$

Where V_1 is volume of solution W, V_2 is the volume of irradiated solution W taken out for incubation, V_3 is the total volume incubated in the dark, ΔA_{510} is the change in absorbance between an irradiated sample and control sample after incubation, l is the pathlength of the cuvette in cm and ε is molar extinction coefficient. The photon flux (q_{in}) was calculated by using the equation given below.

$$q_{in} = \frac{n(Fe^{2+})}{t} \times \Phi\lambda$$

where "$n(Fe^{2+})/t$" represents the slope derived from the plot of $n(Fe^{2+})$ against t, and we utilized a Φ_λ value of 1.19 for an excitation wavelength of 407 nm. The photon flux (q_{in}) found is 4.07×10^{-6} Einstein/min using this equation. The determination of the quantum yield of photodecomposition followed a method outlined in previously published literature.

Photochemical quantum yield calculation

The quantum yield for the photodecomposition of Nap-NO in DMSO/H_2O and Nap-NO in both liposome mixtures was estimated by using the following equation

$$\Phi = \frac{[R]_0 - [R]_t}{T} \times V \times \frac{N_A}{q_{in}} \times \frac{1}{f_m}$$

where N_A is the Avogadro constant, f_m is the mean value of the fraction of light absorbed at time "t", $[R]_0$ and $[R]_t$ are the molar concentrations of R at the beginning and at the end of the irradiation period, V is the volume of the solution, and t is the irradiation time. The blue light source photon flux (q_{in}) was estimated using the well-known procedure.[43]

QUANTIFICATION AND STATISTICAL ANALYSIS

Standard error of the mean is shown on figures unless otherwise noted. The study does not include any specific quantification and statistical analysis.